JBIC Journal of Biological Inorganic Chemistry (2023) 28:571–581
https://doi.org/10.1007/s00775-023-02009-x

ORIGINAL PAPER

meso-Bromination of cyano- and aquacobalamins facilitates their processing into Co(II)-species by glutathione

Ilia A. Dereven'kov[1] · Vladimir S. Osokin[1] · Ilya A. Khodov[2] · Valentina V. Sobornova[2] · Nikita A. Ershov[1] · Sergei V. Makarov[1]

Received: 12 February 2023 / Accepted: 5 July 2023 / Published online: 22 July 2023

Abstract

Cyanocobalamin (CNCbl), a medicinal form of vitamin B_{12}, is resistant to glutathione (GSH), and undergoes intracellular processing via reductive decyanation producing the Co(II)-form of Cbl (Cbl(II)) mediated by the CblC-protein. Alteration of the CblC-protein structure might inhibit CNCbl processing. Here, we showed that introducing a bromine atom to the C10-position of the CNCbl corrin ring facilitates its reaction with GSH leading to the formation of Cbl(II) and cyanide dissociation. In a neutral medium, the reaction between C10-Br-CNCbl and GSH proceeds via the complexation of the reactants further leading to dimethylbenzimidazole (DMBI) substitution and electron transfer from GSH to the Co(III)-ion. The reaction is accelerated upon the GSH thiol group deprotonation. The key factors explaining the higher reactivity of C10-Br-CNCbl compared with unmodified CNCbl towards GSH are increasing the electrode potential of CNCbl two-electron reduction upon meso-bromination and the substantial labilization of DMBI, which was shown by comparing their reactions with cyanide and the pK_a values of DMBI protonation ($pK_{a\ base\text{-}off}$). Aquacobalamin (H_2OCbl) brominated at the C10-position of the corrin reacts with GSH to give Cbl(II) via GSH complexation and subsequent reaction of this complex with a second GSH molecule, whereas unmodified H_2OCbl generates glutathionyl-Cbl, which is resistant to further reduction by GSH.

Graphical abstract

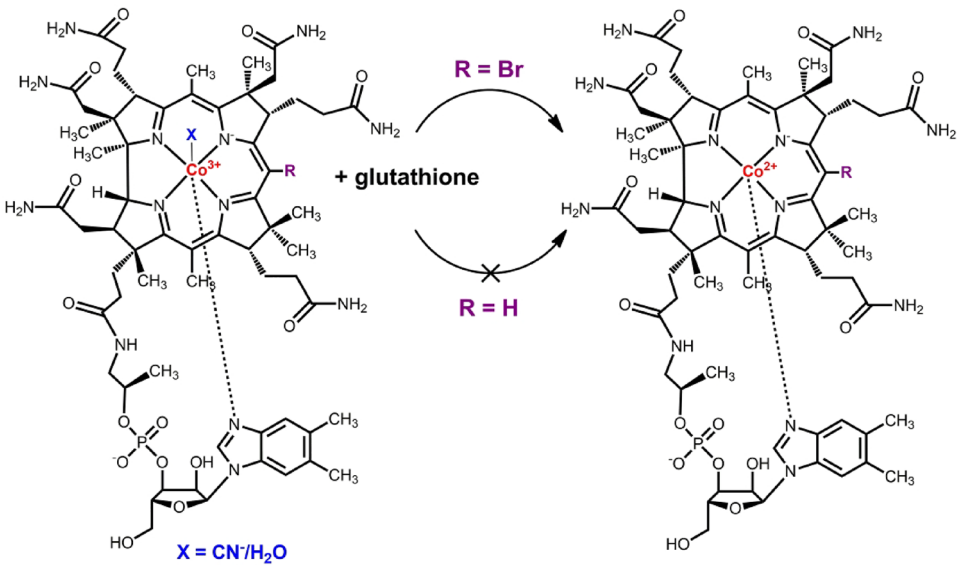

Keywords Vitamin B_{12} · Cyanocobalamin · Aquacobalamin · Glutathione · Reduction · *meso*-Modification

Extended author information available on the last page of the article

Abbreviations

C10-Br-CNCbl	CNCbl brominated at C10-position of corrin ring
C10-Br-H_2OCbl	H_2OCbl brominated at C10-position of corrin ring
Cbi	Cobinamide
Cbl	Cobalamin
CNCbl	Cyanocobalamin
DMBI	5,6-Dimethylbenzimidazole
GSCbl	Glutathionylcobalamin
GSH	Glutathione
H_2OCbl	Aquacobalamin
C10-Br-SO_3Cbl	Sulfitocobalamin brominated at C10-position of corrin ring

Introduction

Cyanocobalamin (CNCbl) is relatively inert in comparison with aquacobalamin. Numerous examples of ligand substitution reactions have been reported to H_2OCbl [1, 2], whereas CNCbl does not react with most of ligands. It is resistant to mild reducing agents and can be reduced to Co(II) and Co(I)-species by $NaBH_4$, Ti(III), Zn [1], and sulfur-containing compounds (e.g., dithionite, sodium hydroxymethanesulfinate [3], and sulfoxylate [1]). Among biological reductants, conversion of CNCbl to one-electron reduced cobalamin (Cbl(II)) is achievable by the hydroquinone form of flavin mononucleotide (FMNH2) [4]. Reactions of CNCbl with FMNH2, dithionite, or hydroxymethanesulfinate proceed via slow dissociation of 5,6-dimethylbenzimidazole nucleotide (DMBI) and faster coordination of the reductant on Co(III) with the subsequent electron transfer [4]. The reduction of CNCbl to Co(II)-form results in its decyanation [5].

Despite the low reactivity of CNCbl, it undergoes efficient intracellular processing to coenzyme species. This process is mediated by CblC-protein, which utilizes flavin mononucleotide to transfer electron from reduced nicotinamide adenine dinucleotide phosphate to Co(III)-ion [6, 7]. The generated Cbl(II) is further used to synthesize methyl- and adenosyl-Cbls. Mutations can cause alterations of the CblC-protein structure, leading to its inability to process CNCbl and other Cbl species [8]. In this case, developing novel Cbl species that CblC-protein can process with an altered structure is important. One of the approaches suggests the application of cysteaminyl- and 2-mercaptopropionylglycino-Cbls, which can repair the activity of pathogenic forms of CblC in contrast to the inactive glutathionyl-Cbl [9].

An alternative approach may utilize modification of Cbl structure (e.g., corrin ring). In this case, introduction of various substituents to the C10-position of the corrin ring can cause changes in the properties of the Co(III)-ion and axial bonds [10–12] and its reactivity toward biological molecules, which, however, remains poorly understood. *meso*-Bromination of CNCbl is a relatively straightforward process: it can be performed in high yield using *N*-bromosuccinimide in glacial acetic acid [13, 14]. C10-chlorination of CNCbl represents a rather more complex task, since most chlorination agents react with Cbls with the formation of C10-chlorinated c-lactone derivatives [15, 16]. Synthesis of C10-brominated aquacobalamin (C10-Br-H_2OCbl) is a more complex process. The first method of C10-Br-H_2OCbl preparation involves (i) alkylation of the Co(III)-ion in CNCbl via its reduction to the Co(I)-form of Cbl (Cbl(I)) and subsequent addition of an alkyl halide, (ii) bromination of the generated organo-Cbl with N-bromosuccinimide, and (iii) photolytic dealkylation of the C10-Br-alkyl-Cbl under aerobic conditions [17]. Another method of C10-Br-H_2OCbl synthesis suggests (i) conversion of C10-Br-CNCbl to C10-Br-phenylethynylCbl in the presence of phenylacetylene, Cu(I) acetate, and 1,8-diazabicyclo[5.4.0]undec-7-ene (DBU) in dimethyl acetamide medium, and dealkylation of C10-Br-phenylethynyl-Cbl in acidic medium [18]. Ligand-exchange reactions involving C10-Br-H_2OCbl have been studied. It was shown that C10-Br-H_2OCbl, as well as C10-Cl-H_2OCbl, reacts more slowly with azide and imidazole than unmodified H_2OCbl, whereas *meso*-halogenation increases equilibrium constants for binding sulfite, azide, and nitrite and decreases the stability of complexes with imidazole 4-*N*,*N*-dimethylaminopyridine [11, 17]. These results were explained by the decrease of charge on the Co(III)-ion due to *meso*-halogenation, whereas the charge on the corrin ring becomes more positive [17]. Halogen atoms in Cbls act as σ-withdrawing substituents and π-donors [19]. *meso*-Halogenation affects axial bond lengths as well. For example, the Co–N(DMBI) bond length increases upon chlorination of CNCbl and chlorination or bromination of H_2OCbl, whereas *meso*-bromination of azido-Cbl causes shortening Co-N(DMBI) bond length [15, 17]. The redox properties of *meso*-halogenated Cbls are almost unexplored: *meso*-halogenation results in a positive shift of the electrode potential of the CNCbl reduction to Cbl(I) [13, 18]. Considering the biological importance of *meso*-halogenated Cbls [13, 20, 21], studies of their reactions with biological substrates represent an important task.

Reactions of Cbls with glutathione (GSH) play an important role in their biochemistry. H_2OCbl tightly binds GSH to give glutathionylcobalamin (GSCbl) [22], which was detected in vivo [23]. GSCbl can be processed by CblC-protein to reduced species utilizing another GSH molecule [24]. GSH is involved in processing of alkyl-Cbls; it attacks the Co(III)-C bond to give Co(I)-species and thioether [25]. Nevertheless, reactions of *meso*-modified Cbls with GSH remain unstudied. Here, we report the results of the study of

the reaction between C10-Br-cyano- and C10-Br-aqua-Cbls and GSH (Fig. 1).

Experimental section

Cyanocobalamin (Sigma-Aldrich; ≥ 98%), hydroxocobalamin hydrochloride (Sigma-Aldrich; ≥ 96%), L-glutathione (J&K; GSH; 99%), potassium cyanide (Sigma-Aldrich; 97%), *N*-bromosuccinimide (Alfa Aesar; 99%), glacial acetic acid (Khimreactiv, Russia), and trifluoroacetic acid (Sigma-Aldrich; 99%) were used without additional purification.

C10-Br-CNCbl was synthesized according to the reported procedure [13], i.e., a slight excess of *N*-bromosuccinimide was slowly added by 0.5 mg portions to CNCbl dissolved in glacial acetic acid. C10-Br-CNCbl was purified by column chromatography on silica gel (Macherey–Nagel Silica 60, 0.04–0.063 mm) using water as eluent and lyophilized. The UV–vis spectrum of the product coincided with that reported in the literature: λ_{max} are 365, 550, and 576 nm (Fig. S1) [13]. The incorporation of a bromine atom in CNCbl was proved by MALDI-MS (Fig. S2). The bromination of the C10-position of the corrin ring is supported by ^{1}H NMR (Figs. S3, S4), i.e., the signal of the C10-proton is lacking in the spectrum of the product. Signals in the ^{1}H NMR spectrum were assigned according to the reported data [26].

C10-Br-H_2OCbl was synthesized using the following procedure: 20 mg of C10-Br-CNCbl was dissolved in an acetate buffer (pH 5) containing 0.1 M sodium sulfite. The solution was incubated at room temperature for 30 min. Generated C10-Br-SO_3Cbl was purified using column chromatography on Macherey–Nagel Silica 60 (0.04–0.063 mm) with water as the eluent. Sodium periodate (10 mg) was added to the purified C10-Br-SO_3Cbl, and C10-Br-H_2OCbl was formed almost immediately. C10-Br-H_2OCbl was then purified by column chromatography on Macherey–Nagel Silica 60 (0.04–0.063 mm), with the column being continuously washed with water and then by aqueous ethanol (60%). C10-Br-H_2OCbl was finally eluted by aqueous acetic acid (10%) and lyophilized. The UV–vis spectrum of the product coincided with that reported in the literature, with λ_{max} at 356, ca. 535, and 554 nm (Fig. S1). The incorporation of a bromine atom in H_2OCbl was proved by MALDI-MS (Fig. S2) and the presence of a bromine atom in the C10-position of the corrin ring was supported by ^{1}H NMR (Figs. S5, S6). The identity of C10-Br-H_2OCbl was supported by a comparison of characteristic chemical shifts with the literature data (Table S1).

CNCbi was synthesized using a published procedure [27]. The UV–vis spectrum of the product coincided with that reported in the literature: λ_{max} were 353, 496, and 528 nm (Fig. S1) [28]. The absence of DMBI was supported by MALDI-MS (Fig. S2). The same protocol was employed for synthesizing C10-Br-CNCbi with the use of C10-Br-CNCbl as starting complex. C10-Br-CNCbi was purified by column chromatography on silica gel (Macherey–Nagel Silica 60, 0.04–0.063 mm): the column was continuously washed with water, then diluted acetic acid (0.1%). C10-Br-CNCbi was finally eluted with aqueous acetic acid (10%) and lyophilized. λ_{max} were 359, 524, and 548 nm (Fig. S1). The incorporation of the bromine atom and the absence of DMBI in C10-Br-CNCbi were proved by MALDI-MS (Fig. S2).

Buffer solutions (phosphate, borate, and carbonate; 0.1 M) were used to maintain pH during the measurements. The pH values of the solutions were determined using the Multitest IPL-103 pH-meter (SEMICO) equipped with the ESK-10601/7 electrode (Izmeritelnaya tekhnika) filled with 3.0 M KCl solution. The electrode was preliminarily calibrated using standard buffer solutions (pH 1.65–12.45). In a strongly acidic medium, pH values were adjusted by adding exact quantities of trifluoroacetic acid and calculated using its pK_a = 0.25 (25.0 °C) [29].

Ultraviolet–visible (UV–vis) spectra were recorded on a cryothermostated (± 0.1 °C) Cary 50 UV–vis or Shimadzu UV-1800 spectrophotometers in quartz cells under anaerobic conditions. The kinetics of the reaction between

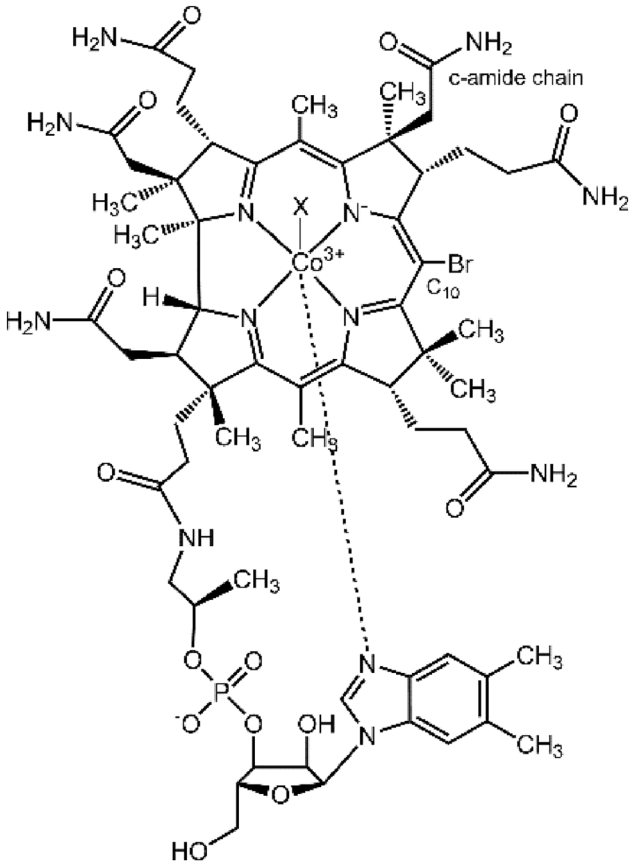

Fig. 1 The chemical structure of C10-Br-CNCbl

C10-Br-CNCbl and cyanide was studied on a thermostated (± 0.1 °C) RX2000 (Applied Photophysics, UK) rapid mixing stopped-flow accessory connected to the Cary 50 spectrophotometer. Experimental data were analyzed using Origin 9.1 software.

NMR measurements were performed on a Bruker Avance III 500 NMR spectrometer in D_2O (Cambridge Isotope Laboratories Inc.; 99.9%). The spectral width of the NMR was 7 kHz, and the spectral resolution was 0.222 Hz. The total number of data points acquired was 32,768, with a total acquisition time of 4 min. The WATERGATE [30] sequence is a pulse sequence designed to suppress the signal from water molecules in ^{1}H NMR spectra. It consists of a W5 train, a series of five pulses, followed by a 213 µs binomial delay. The W5 train is designed to create a strong magnetization transfer from the water molecules to other molecules in the sample. At the same time, the binomial delay helps to further reduce the signal from water. This sequence can be used to improve the signal-to-noise ratio of ^{1}H NMR spectra and to make it easier to identify and quantify the signals from other molecules in the sample. The 1D NMR spectra were processed using various techniques, including exponential decay multiplication to 0.3 Hz, zero filling, line broadening, and baseline correction.

MALDI-MS measurements were performed on a Shimadzu AXIMA Confidence mass-spectrometer with 2,5-dihydroxybenzoic acid as the matrix for Cbl species. Mass spectra of Cbi species were collected in the absence of a matrix.

Cyclic voltammetry experiments were carried out using an Elins R-20H potentiostat–galvanostat (Electro Chemical Instruments, Russia). A conventional three electrode arrangement consisting of a glassy carbon working electrode, a platinum wire as the counter electrode, and a silver chloride (in 4.2 M KCl) reference electrode (0.202 V vs NHE at 20 °C) was employed. The scan rate was 100 mV/s. Before the measurements, the surface of the glassy carbon electrode was polished with alumina powder and phosphate buffer (0.1 M) was used as the supporting electrolyte.

Results and discussion

Adding GSH (20 mM) to CNCbl in a neutral medium and incubating the mixture for two hours does not result in noticeable changes in the UV–vis spectrum. At pH 11.2, changes in the UV–vis spectrum upon incubation of CNCbl with GSH (5 mM) become more pronounced (Fig. S7), i.e., maxima at 312 and 478 nm emerge indicating the formation of Cbl(II). These results can be explained by the generation of thiolate species (GS^-; pK_a for deprotonation of thiol group of GSH is 8.9 at 25.0 °C [31]), which substitute DMBI in CNCbl to give an unstable CNCbl-$^-$SG complex that decomposes to Cbl(II), CN^- and a thiyl radical. To support this mechanism, GSH was added to aquacyano cobinamide (H_2O)(CN)Cbi, a nucleotide-free derivative of CNCbl. The first step of the reaction proceeds upon mixing of the reactants, i.e. new maxima at 314, 367, 470, 539 and 580 nm emerge (Fig. S8), which can be attributed to the mixture of the Co(II)-form of Cbi (Cbi(II); maxima at 314 and 470 nm [32]) and dicyano-Cbi (maxima at 367, 539 and 580 nm [33]; $(CN)_2$Cbi). The second step is accompanied by a slow decrease of absorbance at 367, 539 and 580 nm (Fig. S8) indicating the reduction of $(CN)_2$Cbi to Cbi(II). Thus, (H_2O)(CN)Cbi rapidly reacts with GSH with the formation of Cbi(II) and CN^-, which further binds with the remaining (H_2O)(CN^-)Cbi to give $(CN)_2$Cbi. Subsequent reaction between $(CN)_2$Cbi and GSH proceeds at a slow rate. Therefore, substituting DMBI by GSH is a key step in the course of CNCbl reduction by GSH, which is unavailable at physiological pH.

In contrast to CNCbl, the addition of GSH (20 mM) to C10-Br-CNCbl in a neutral medium is accompanied by the slow formation of species with maxima at 318 and 485 nm (Fig. 2A). The UV–vis spectrum of the reaction product resembles that of Cbl(II), although the maxima of Cbl(II) are blue-shifted compared to the brominated species. The formation of paramagnetic Co(II)-species is supported by ^{1}H NMR (Fig. 3): the incubation of C10-Br-CNCbl with an excess of GSH leads to a gradual disappearance of all signals attributed to Cbl. Adding an aerobic solution of CN^- to C10-Br-CNCbl after the reaction with GSH leads to the formation of species identical to C10-Br-$(CN)_2$Cbl (Fig. S9). Thus, the bromine atom remains in the corrin structure after the reaction with GSH, and the reaction between GSH and C10-Br-CNCbl produces C10-Br-Cbl(II).

We studied the kinetics of the reaction between C10-Br-CNCbl and an excess of GSH. At pH 7.4, the typical kinetic curve of the reaction is described by an exponential equation (Fig. 2A) indicating first order with respect to C10-Br-CNCbl. The dependence of the observed rate constant ($k_{obs.}$) on GSH concentration is nonlinear and reaches a plateau at [GSH] > 10 mM (Fig. 2B). This can be explained by the complexation between C10-Br-CNCbl and GSH prior to electron transfer from GSH to Co(III).

^{1}H NMR followed the reaction between C10-Br-CNCbl and GSH (10 mM) at pH 6.4, a powerful tool for determining the kinetic parameters [34–36]. Typical kinetic curves of the reaction collected using the decay of signals in various regions of ^{1}H NMR spectra (Fig. 3; S10) are described by an exponential equation, and their fitting produces $k_{obs.} = (1.3 \pm 0.2) \cdot 10^{-4}$ s^{-1}, which agrees with the value obtained using UV–vis data [$k_{obs.} = (1.0 \pm 0.1) \cdot 10^{-4}$ s^{-1}]. It

is important to note that after mixing with GSH, signals of C10-Br-CNCbl in the aromatic region are shifted from 6.21, 6.36, 6.97, and 7.15 ppm to 6.27, 6.41, 7.03, and 7.21 ppm, which supports complexation between the reactants.

To elucidate additional mechanistic details of the reaction between C10-Br-CNCbl and GSH, we studied the reaction between C10-Br-CNCbl and CN^- in a basic medium (pH 11.2) to convert cyanide to its deprotonated form ($pK_a = 9.2$ at 25.0 °C [37]). This process leads to the formation of C10-Br-$(CN)_2$Cbl, which exhibits absorption maxima at 370, 562 and 603 nm (Fig. 4A). A typical kinetic curve is described by an exponential equation (Fig. 4A) and the observed rate constant exhibits saturation behavior versus CN^- concentration (Fig. 4B). Similar kinetic features have been reported for the reaction between unmodified CNCbl and CN^-, and Scheme 1 and Eq. (1) have been suggested [38].

$$k_{\text{obs.}} = \frac{k_1 k_2 [CN^-] + k_{-1} k_{-2}}{k_{-1} + k_2 [CN^-]} \quad (1)$$

where k_1, k_{-1}, k_2 and k_{-2} are rate constants corresponding to the step presented by Scheme 1.

Fitting the dependence presented in Fig. 4B to Eq. (1) gives values $k_1 = (0.12 \pm 0.01)\ s^{-1}$, $k_{-2} = (2.0 \pm 0.1) \cdot 10^{-5}\ s^{-1}$, and $k_2/k_{-1} = (55 \pm 3)\ M^{-1}$ (25.0 °C). For unmodified CNCbl, these values are $k_1 = 0.042\ s^{-1}$, $k_{-2} = 7 \cdot 10^{-5}\ s^{-1}$, and $k_2/k_{-1} = 37\ M^{-1}$ (25.0 °C) [38]. These results show that *meso*-bromination of CNCbl leads to labilization of DMBI and increases its affinity towards CN^-, which agrees with earlier observations indicating that C10-Br-H_2OCbl is more reactive towards anionic ligands and less reactive towards neutral bases in comparison with native H_2OCbl [17].

To further support the labilization of DMBI in C10-Br-CNCbl, we determined the $pK_{a\ \text{base-off}}$ of this brominated species (see Scheme 2). We found that new maxima in the UV–vis spectrum at 361, 523, and 551 nm emerged upon acidification of the solution (Fig. 5). These maxima were relatively close to those of C10-Br-monocyanocobinamide (C10-Br-CNCbi; λ_{max}: 359, 524 and 548 nm, Fig. S11), a nucleotide-free analog of C10-Br-CNCbl, which supports the formation of the base-off species of C10-Br-CNCbl in acidic medium. Fitting the dependence of absorbance at 576 nm on pH to Eq. (2) provided a value of $pK_{a\ \text{base-off}} = (1.1 \pm 0.1)$ (25.0 °C; $I = 0.2$ M). This value was noticeably higher than the $pK_{a\ \text{base-off}}$ of CNCbl (0.1) [39, 40], which supports the labilization of DMBI upon *meso*-bromination of CNCbl.

$$A = A_1 + (A_2 - A_1) \frac{10^{pH}}{10^{pH} + 10^{pK_{\text{abase-off}}}} \quad (2)$$

A, A_1 and A_2 are the absorbances at the monitoring wavelength for the compound at a particular pH, for the protonated species, and for the deprotonated species, respectively.

The rate constant of DMBI dissociation (0.12 s^{-1}) is significantly higher than the rate constant on the plateau of dependence presented by Fig. 2B (ca. $2 \cdot 10^{-4}\ s^{-1}$). We suggest that the complexation between reactants initiates the reaction without substituting axial ligands. For the reaction between C10-Br-CNCbl and GSH at pH 7.4, the mechanism presented by Scheme 3 can be suggested. The complexation between CNCbl and GSH facilitates deprotonation of the

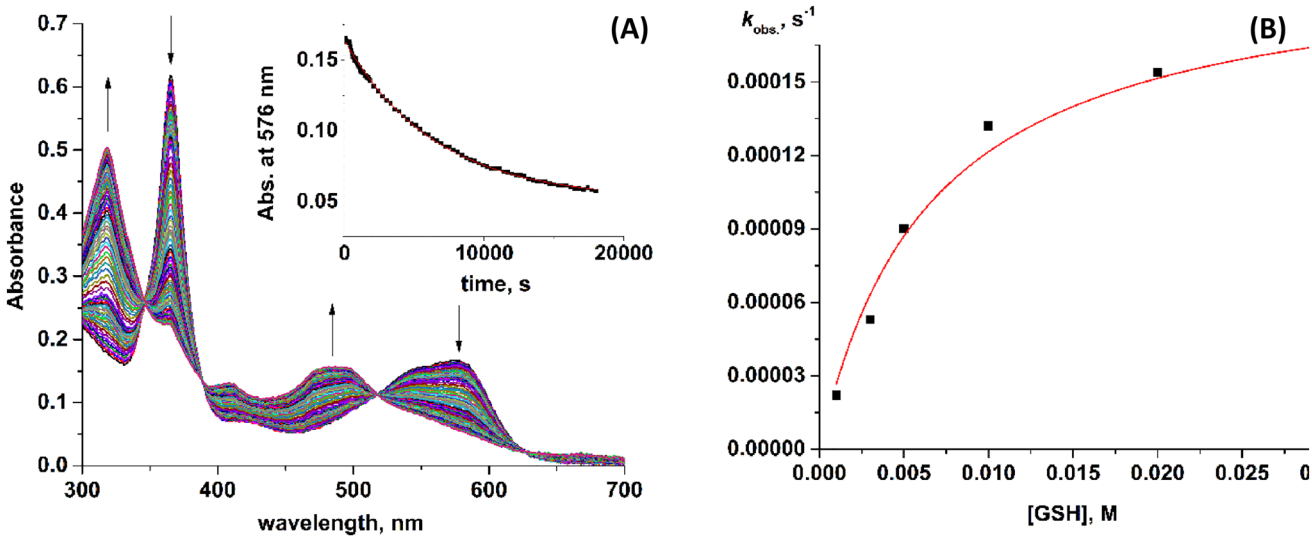

Fig. 2 **A** UV–vis spectra of the reaction between C10-Br-CNCbl ($2.3 \cdot 10^{-5}$ M) and GSH (2.0 10^{-2} M) at pH 7.4, 25.0 °C. Inset: a kinetic curve of the reaction; **B** dependence of the observed rate constant ($k_{\text{obs.}}$) on [GSH]

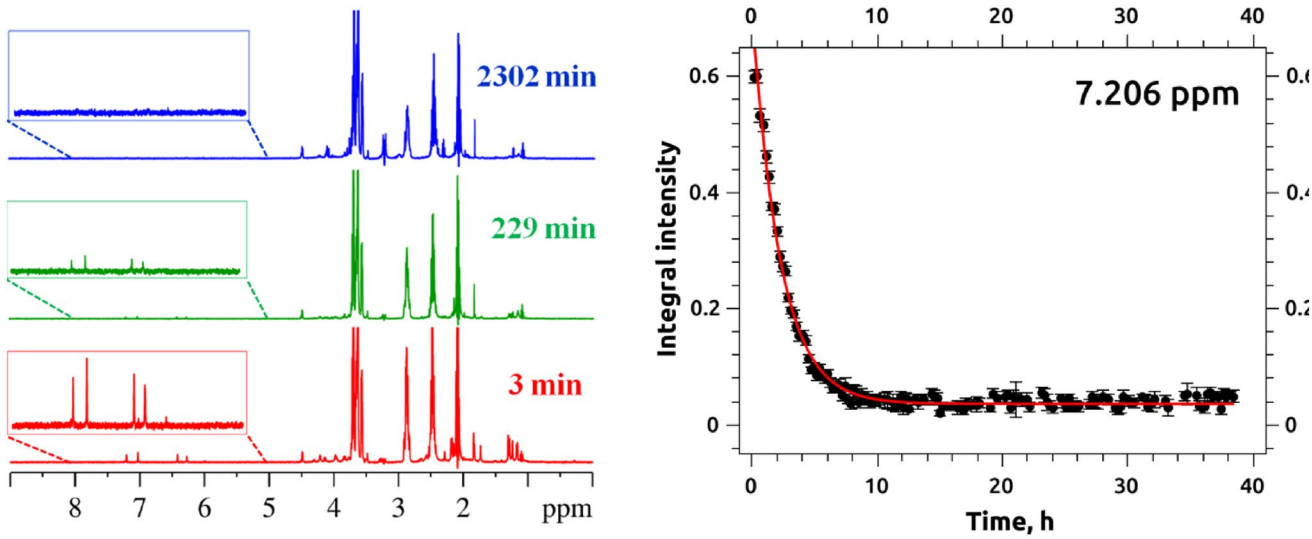

Fig. 3 (Left panel) ^{1}H NMR spectra recorded during the reaction between C10-Br-CNCbl ($7.0\cdot10^{-4}$ M) and GSH ($1.0\cdot10^{-2}$ M) at pH 6.4, room temperature. (Right panel) The kinetic curve of the reaction was monitored using the integral intensity of the NMR signals at 7.2 ppm fitted to an exponential equation ($k_{obs.} = 1.3\cdot10^{-4}$ s^{-1}; $R^2 = 0.997$)

thiol group of GSH, and further DMBI substitution. The complex Co(III)-$^{-}$SG is unstable and decomposes to the thiyl radical and the Co(II)-form of C10-Br-CNCbl, which results in its decyanation.

For Scheme 3, Eq. 3 can be suggested:

$$k_{obs.} = \frac{k_{sub.}K_{compl.}[GSH]}{1 + K_{compl.}[GSH]}, \quad (3)$$

where $K_{compl.}$ is the equilibrium constant for GSH binding by C10-Br-CNCbl, M^{-1}; $k_{sub.}$ is the rate constant for DMBI substitution upon rearrangement of C10-Br-CNCbl-GSH complex. Fitting the plot presented by Fig. 2B to Eq. (3) gives values $K_{compl.} = (100 \pm 14)$ M^{-1} and $k_{sub.} = (2.4 \pm 0.3)\cdot10^{-4}$ s^{-1} (pH 7.4, 25.0 °C).

Further, we studied the kinetics of the reaction between C10-Br-CNCbl and GSH at different pHs. In alkaline medium, the reaction produces C10-Br-Cbl(II) as in neutral solutions. However, the process proceeds more

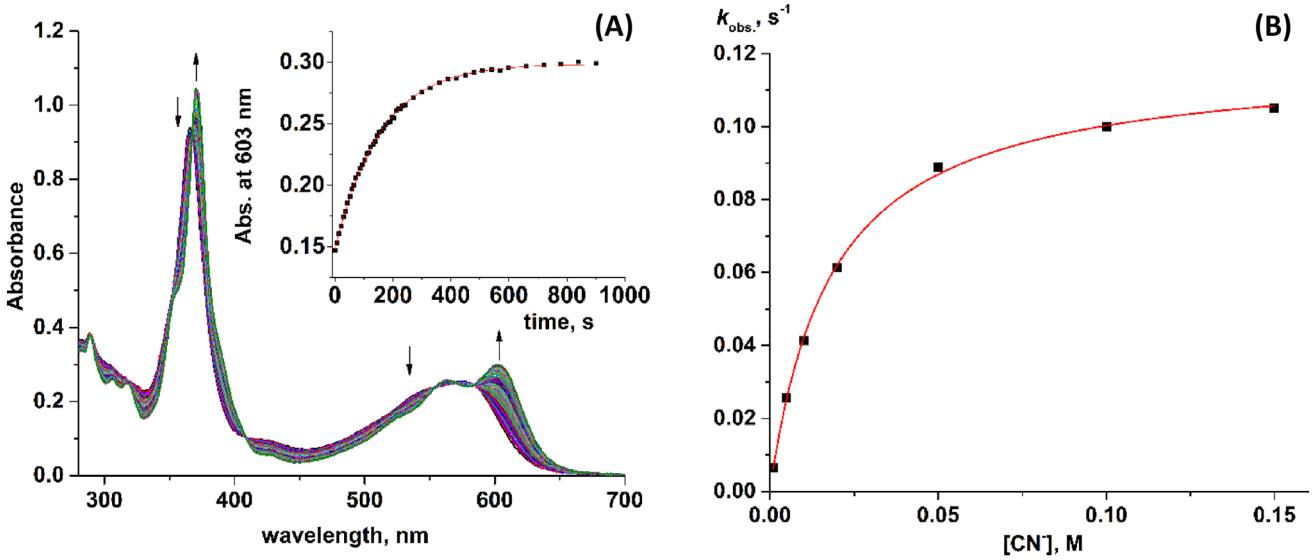

Fig. 4 **A** UV–vis spectra of the reaction between C10-Br-CNCbl ($3.5\cdot10^{-5}$ M) and CN$^-$ ($1.0\cdot10^{-3}$ M) at pH 11.2, 25.0 °C. Inset: a kinetic curve of the reaction; **B** dependence of the observed rate constant of the reaction on cyanide concentration fitted to Eq. (1)

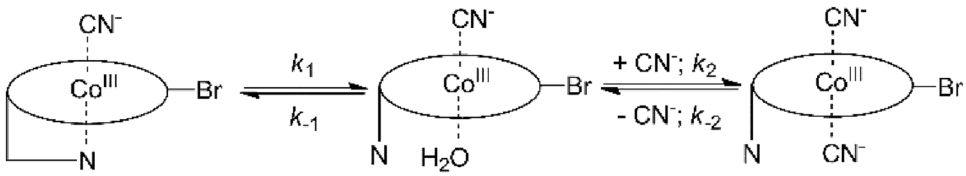

Scheme 1 The mechanism of the reaction between CNCbl and CN^-

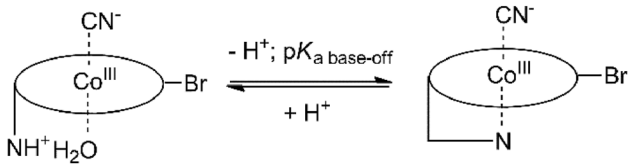

Scheme 2 Protonation of DMBI of C10-Br-CNCbl in aqueous solutions

rapidly and the profile of the kinetic curve becomes typical of an autocatalytic reaction (Figs. S13, S13). The origin of the autocatalytic behavior is unclear, although it could be due to further reactions involving the thiyl radical formed in the course of GSH oxidation. The dependence of the rate of C10-Br-CNCbl reduction by GSH on pH is shown in Fig. 6, which demonstrates an increase in the rate (pH 6…9.2), and a further slight decrease (pH 9.2…11.2). This can be explained by the deprotonation of the thiol group that accelerates DMBI substitution in C10-Br-CNCbl, and by the deprotonation of the NH_3^+-group ($pK_a = 9.3$ at 25.0 °C [31]) that generates a species slightly less reactive than the thiolate with a protonated amino group.

Taking into account Scheme 3 and the presence of two reaction pathways involving C10-Br-CNCbl reduction by GS^- species with (1) protonated and (2) deprotonated amino group, Eq. (4) can be deduced (note, it is valid only at [GSH] < ca. 5 mM).

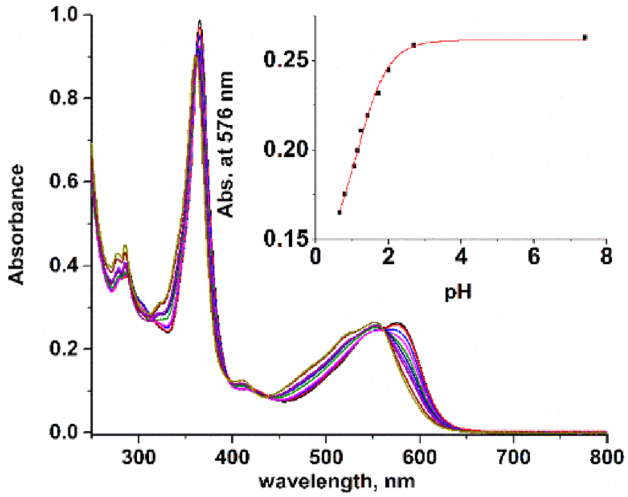

Fig. 5 UV–vis spectra of C10-Br-CNCbl ($3.5 \cdot 10^{-5}$ M) collected at different pH at 25.0 °C, $I = 0.2$ M ($NaNO_3$). Inset: a plot of absorbance at 576 nm versus pH fitted to Eq. (2)

$$k_{obs.} = \frac{k_{sub.(1)} \bullet K_{compl.(1)} \bullet [GSH]}{1 + 10^{-pH+pK_{a1}} + 10^{pH-pK_{a2}}} + \frac{k_{sub.(2)} \bullet K_{compl.(2)} \bullet [GSH]}{1 + 10^{-2pH+pK_{a1}+pK_{a2}} + 10^{-pH+pK_{a2}}} \quad (4)$$

where pK_{a1} and pK_{a2} correspond to deprotonation of thiol and amino groups of GSH bound in complex with C10-Br-CNCbl, respectively; $k_{sub.(1)}$ and $k_{sub.(2)}$ are the rate constants for DMBI substitution by GS^- species with protonated

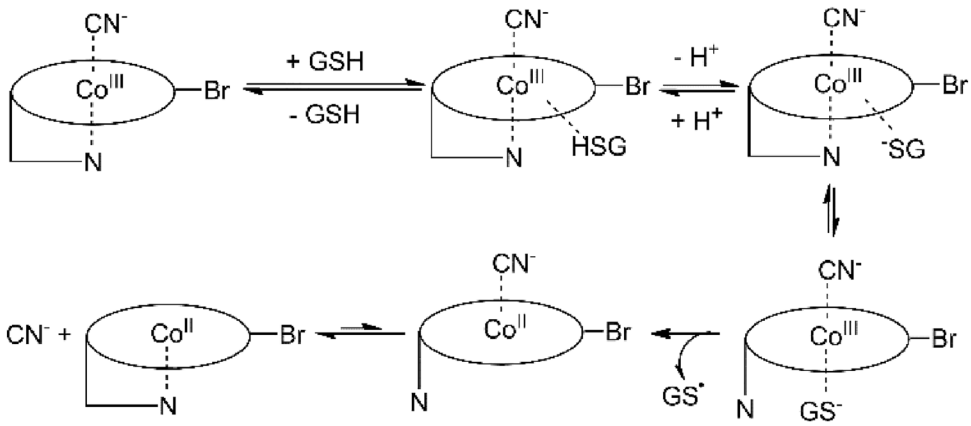

Scheme 3 The mechanism of the reaction between C10-Br-CNCbl and GSH in a neutral medium

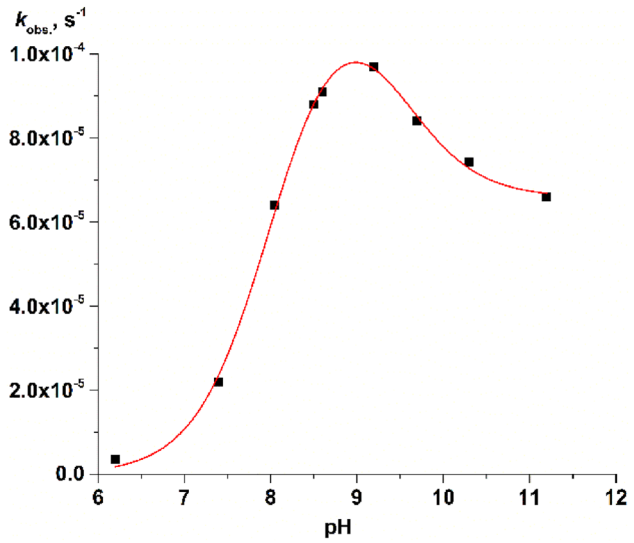

Fig. 6 The plot of the observed rate constant of the reaction between C10-Br-CNCbl ($3.5\cdot10^{-5}$ M) and GSH ($1.0\cdot10^{-3}$ M) at 25.0 °C versus pH fitted to Eq. (4)

(1) and deprotonated (2) amino groups, s^{-1}; $K_{compl.(1)}$ and $K_{compl.(2)}$ are the equilibrium constants for complexation between C10-Br-CNCbl and GSH species with protonated (1) and deprotonated (2) amino groups, M^{-1}. Fitting the data presented by Fig. 6 to Eq. (4) gives values $pK_{a1} = (8.0 \pm 0.1)$, $pK_{a2} = (9.4 \pm 0.1)$, $K_{compl.(1)}\ k_{sub.(1)} = (0.12 \pm 0.01)\ M^{-1}\ s^{-1}$ and $K_{compl.(2)}\ k_{sub.(2)} = (6.6 \pm 0.2)\cdot10^{-2}\ M^{-1}\ s^{-1}$. The determined value of pK_{a2} excellently agrees with literature data for free GSH ($pK_a = 9.3$ [31]), however, pK_{a1} is notably lower than pK_a of the thiolate group of unbound GSH ($pK_a = 8.9$ [31]). Thus, binding GSH with C10-Br-CNCbl facilitates the formation of thiolate species and does not affect amino group deprotonation.

A bromine atom in Cbls acts as a σ-electron withdrawing group and affects their electrode potentials. In the case of CNCbl, *meso*-bromination shifts the potential of the CNCbl/Cbl(I) couple as well, i.e., − 0.97 V (vs. Ag/AgCl at pH 6.9, 25.0 °C (Fig. S14); − 0.76 V vs. normal hydrogen electrode, NHE, at 22 °C in DMSO/isopropanol mixture [5]) and − 0.87 V (vs. Ag/AgCl at pH 6.9, 25.0 °C (Fig. S15); − 0.80 V vs. $K_3[Fe(CN)_6]$ at pH 8 [13]) for CNCbl and C10-Br-CNCbl, respectively. These results indicate that the base-on and base-off species of C10-Br-CNCbl exhibit more pronounced electron-withdrawing properties than unmodified ones, which may favor its reduction by GSH, alongside with the labilization of DMBI.

Intracellular reactions between C10-Br-CNCbl and GSH producing Co(II)-species may be followed by subsequent oxidation of C10-Br-Cbl(II) to C10-Br-H_2OCbl. It is well known that the reaction between H_2OCbl and GSH produces glutathionylcobalamin [22], which possesses high stability in the presence of GSH excess (Fig. S16). We examined the reaction between C10-Br-H_2OCbl and GSH to evaluate the stability of C10-Br-GSCbl. For synthesizing C10-Br-H_2OCbl, we employed a novel protocol including substitution of cyanide in C10-Br-CNCbl by sulfite (Fig. S17), and subsequent oxidation of C10-brominated sulfitocobalamin by periodate (Fig. S18). We found that adding sulfite to C10-Br-CNCbl in a weakly acidic medium resulted in the formation of sulfito-species (Fig. S17). C10-Br-SO_3Cbl was purified from cyanide and excess sulfite using column

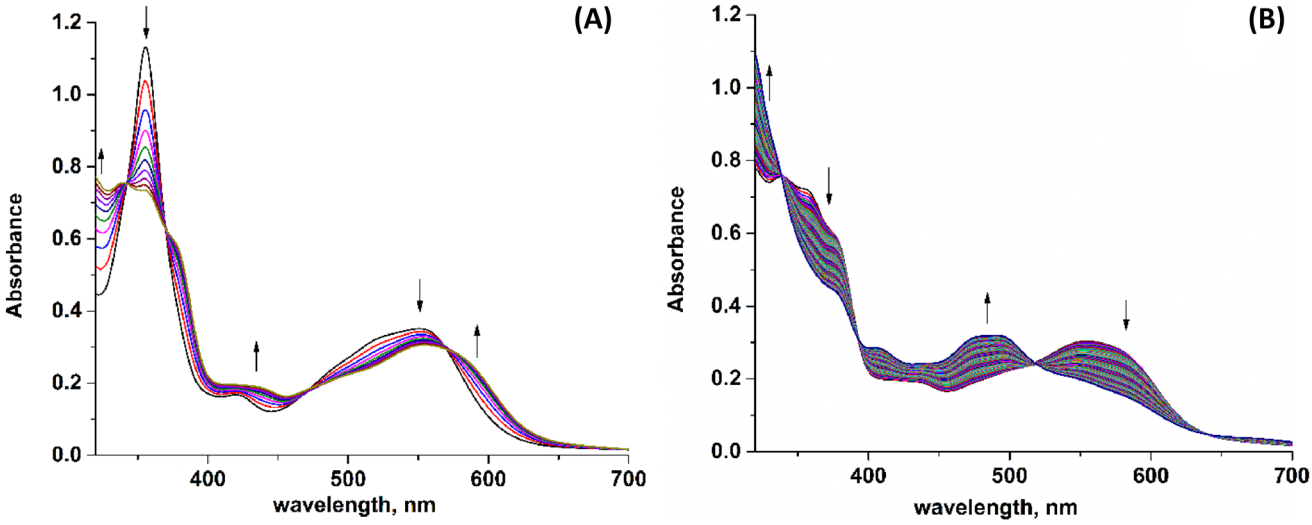

Fig. 7 UV–vis spectra of the first (**A**) and second (**B**) steps of the reaction between C10-Br-H_2OCbl ($5.0\cdot10^{-5}$ M) and GSH ($5.0\cdot10^{-4}$ M) at pH 6.2, 25.0 °C with a time interval of 60 s

chromatography, and the bound sulfite was oxidized to give an uncoordinating on Co(III) sulfate species (Fig. S18). For this purpose, periodate is the best choice due to its high reactivity to sulfite and inertness to corrin and side chains in weakly acidic, neutral, and alkaline media [41].

The addition of GSH to C10-Br-H_2OCbl results in reactions accompanied by changes in the UV–vis spectrum presented in Fig. 7; species with maxima at 340, 554, and 585 nm are generated in the course of the first step, which is further transformed to C10-Br-Cbl(II). Apparently, the first step corresponds to the GSH binding by the Co(III)-ion and is characterized by first orders with respect to GSH and C10-Br-H_2OCbl (Figs. S19, S20), with a rate constant of (9.1 ± 0.3) $M^{-1} \cdot s^{-1}$ (pH 6.2, 25.0 °C). For unmodified H_2OCbl, the formation of GSCbl proceeds approximately twofold more rapidly [22], which agrees with earlier reports of lower reactivity of C10-Br-H_2OCbl toward neutral ligands in comparison with native H_2OCbl [17]. The reaction between C10-Br-GSCbl and GSH is also characterized by first orders with respect to both reactants (Figs. S19, S20) with a rate constant of (0.37 ± 0.02) $M^{-1} \cdot s^{-1}$ (pH 6.2, 25.0 °C). Unmodified GSCbl is relatively stable in the presence of GSH (Fig. S16). Therefore, the C10-bromination of H_2OCbl destabilizes its complex with GSH.

The main reason for the destabilization can be an increase in the potential of the Co(III)/Co(II) couple upon the introduction of a σ-electron withdrawing bromine atom. We collected cyclic voltammograms for unmodified and C10-brominated Cbl species to support this suggestion. Figures S21 and S22 show that cyclic voltammograms for H_2OCbl and C10-Br-GSCbl include two reductions and corresponding two oxidation events for both complexes, which can be attributed to the $H_2OCbl(III)_{base\text{-}on}$/$Cbl(II)_{base\text{-}on}$ and $Cbl(II)_{base\text{-}on}$/Cbl(I) couples. For unmodified H_2OCbl, the potentials for the $H_2OCbl(III)_{base\text{-}on}$/$Cbl(II)_{base\text{-}on}$ and $Cbl(II)_{base\text{-}on}$/Cbl(I) couples are + 0.01 and -0.83 V (vs. Ag/AgCl; pH 6.9, 25 °C), respectively. Note that the literature values for these couples are + 0.20 and − 0.61 V (vs. NHE; 22 °C) [42]. For C10-Br-H_2OCbl, the potentials for the $H_2OCbl(III)_{base\text{-}on}$/$Cbl(II)_{base\text{-}on}$ and $Cbl(II)_{base\text{-}on}$/Cbl(I) couples are + 0.08 and − 0.72 V (vs. Ag/AgCl; pH 6.9, 25 °C), respectively. Thus, *meso*-bromination of H_2OCbl shifts the potentials to a more positive direction, i.e., C10-Br-H_2OCbl possesses more pronounced electron-withdrawing properties than H_2OCbl, which can lead to polarization of the Co(III)-S bond and increase its reactivity towards a second GSH molecule. It is important to note that reducing *meso*-brominated Cbl species can result in their debromination [43]. However, cyclic voltammogram of C10-Br-H_2OCbl indicates the presence of two clear quasi-reversible processes assuming the absence of bromine atom loss upon electrochemical formation of Co(II) and Co(I)-species, although we observed debromination of C10-Br-H_2OCbl and C10-Br-CNCbl upon their reduction by Zn or $NaBH_4$. Thus, the mechanism of corrin ring debromination requires further elaboration.

Conclusions

In this work, we showed that modification of the corrin ring of cyano- and aquacobalamins at the C10-position can alter their reactivity towards glutathione. This structural modification can be significant for the development of novel therapeutic vitamin B_{12} species for patients with pathogenic forms of CblC-protein, which can be processed to uniform Co(II)-species and subsequently utilized for the synthesis of cofactor forms. We proved that *meso*-brominated CNCbl slowly reacts with GSH to give *meso*-brominated Cbl(II) in contrast to unmodified CNCbl, which is resistant to GSH in a neutral medium. At pH 7.4, the reaction between C10-Br-CNCbl and GSH involves complexation of the reactants, leading to DMBI substitution and rapid electron transfer from GSH to the Co(III)-ion. *meso*-Bromination increases the potential of the CNCbl/Cbl(I) couple and labilizes the Co(III)-N(DMBI) bond, i.e., the $pK_{a\ base\text{-}off}$ shifts from 0.1 to 1.1 (25 °C), and the rate constant of DMBI dissociation increases from 0.042 to 0.12 s^{-1} (25 °C). In the case of *meso*-brominated H_2OCbl, the complex formed with GSH can react with the second GSH molecule, generating brominated Cbl(II), whereas unmodified glutathionylcobalamin does not react with GSH.

Supplementary Information The online version contains supplementary material available at https://doi.org/10.1007/s00775-023-02009-x.

Acknowledgements This research was funded by the Russian Science Foundation (Project no. 19-73-00147) to IAD. MALDI-mass-spectrometry experiments were carried out using the resources of the Center for Shared Use of Scientific Equipment of the ISUCT (with the support of the Ministry of Science and Higher Education of Russia, Grant No. 075-15-2021-671).

Author contributions IAD was responsible for investigation, funding acquisition, and writing—original draft preparation. VSO, IAK, VVS, and NAE were responsible for investigation. SVM was responsible for supervision, and writing—review & editing.

Declarations

Conflict of interest The authors declare no conflict of interest.

References

1. Dereven'kov IA, Salnikov DS, Silaghi-Dumitrescu R, Makarov SV, Koifman OI (2016) Redox chemistry of cobalamin and its

derivatives. Coord Chem Rev 309:68–83. https://doi.org/10.1016/j.ccr.2015.11.001
2. Salnikov DS, Kucherenko PN, Dereven'kov IA, Makarov SV, van Eldik R (2014) Kinetics and mechanism of the reaction of hydrogen sulfide with cobalamin in aqueous solution. Eur J Inorg Chem. https://doi.org/10.1002/ejic.201301340
3. Salnikov DS, Dereven'kov IA, Artyushina EN, Makarov SV (2013) Interaction of cyanocobalamin with sulfur-containing reducing agents in aqueous solutions. Russ J Phys Chem A 87:44–48. https://doi.org/10.1134/S0036024413010226
4. Dereven'kov IA, Ugodin KA, Makarov SV (2021) Mechanism of the reaction between cyanocobalamin and reduced flavin mononucleotide. Russ J Phys Chem A 95:2020–2024. https://doi.org/10.1134/S003602442110006X
5. Lexa D, Savéant JM, Zickler J (1980) Electrochemistry of vitamin B12. 5. Cyanocobalamins. J Am Chem Soc 102:2654–2663. https://doi.org/10.1021/ja00528a023
6. Kim J, Gherasim C, Banerjee R (2008) Decyanation of vitamin B_{12} by a trafficking chaperone. Proc Natl Acad Sci USA 105:14551–14554. https://doi.org/10.1073/pnas.0805989105
7. Koutmos M, Gherasim C, Smith JL, Banerjee R (2011) Structural basis of multifunctionality in a vitamin B_{12}-processing enzyme. J Biol Chem 286:29780–29787. https://doi.org/10.1074/jbc.M111.261370
8. Esser AJ, Mukherjee S, Dereven'kov IA, Makarov SV, Jacobsen DW, Spiekerkoetter U, Hannibal L (2022) Versatile enzymology and heterogeneous phenotypes in cobalamin complementation type C disease. IScience 25:104981. https://doi.org/10.1016/j.isci.2022.104981
9. Wingert V, Mukherjee S, Esser AJ, Behringer S, Tanimowo S, Klenzendorf M, Derevenkov IA, Makarov SV, Jacobsen DW, Spiekerkoetter U, Hannibal L (2021) Thiolatocobalamins repair the activity of pathogenic variants of the human cobalamin processing enzyme CblC. Biochimie 183:108–125. https://doi.org/10.1016/j.biochi.2020.10.006
10. Wierzba AJ, Wincenciuk A, Karczewski M, Vullev VI, Gryko D (2018) *meso*-Modified cobalamins: synthesis, structure, and properties. Chem Eur J 24:10344–10356. https://doi.org/10.1002/chem.201801807
11. Knapton L, Marques HM (2005) Probing the nature of the Co(III) ion in cobalamins: a comparison of the reaction of aquacobalamin (vitamin B_{12a}) and aqua-10-chlorocobalamin with some anionic and *N*-donor ligands. Dalton Trans. https://doi.org/10.1039/B416083E
12 Marques HM (2023) The inorganic chemistry of the cobalt corrinoids—an update. J Inorg Biochem 242:112154. https://doi.org/10.1016/j.jinorgbio.2023.112154
13. Prieto L, Rossier J, Derszniak K, Dybas J, Oetterli RM, Kottelat E, Chlopicki S, Zelder F, Zobi F (2017) Modified biovectors for the tuneable activation of anti-platelet carbon monoxide release. Chem Commun 53:6840–6843. https://doi.org/10.1039/C7CC03642F
14. Wagner F (1965) Reactions of the cyano and alkyl cobalamins. Proc Royal Soc A 288:344–347. https://doi.org/10.1098/rspa.1965.0225
15. Brown KL, Cheng S, Zou X, Zubkowski JD, Valente EJ, Knapton L, Marques HM (1997) *Cis* effects in the cobalt corrins. 1. Crystal structures of 10-chloroaquacobalamin perchlorate, 10-chlorocyanocobalamin, and 10-chloromethylcobalamin. Inorg Chem 36:366–3675. https://doi.org/10.1021/ic9615077
16 Dereven'kov IA, Osokin VS, Hannibal L, Makarov SV, Khodov IA, Koifman OI (2021) Mechanism of cyanocobalamin chlorination by hypochlorous acid. J Biol Inorg Chem 26:427–434. https://doi.org/10.1007/s00775-021-01869-5
17. Ghadimi N, Perry CB, Fernandes MA, Govender PP, Marques HM (2015) Probing the nature of the Co(III) ion in cobalamins: the reactions of aquacobalamin (vitamin B_{12a}), aqua-10-chlorocobalamin and aqua-10-bromocobalamin with anionic and neutral ligands. Inorg Chim Acta 436:29–38. https://doi.org/10.1016/j.ica.2015.07.019
18. Brenig C, Mosberger L, Baumann K, Blacque O, Zelder F (2021) Redox-neutral syntheses and electrochemical studies of 10-bromo-substituted light-stable antivitamin B_{12} candidates. Helv. Chim. Acta 104:e2100067. https://doi.org/10.1002/hlca.202100067
19. Navizet I, Perry CB, Govender PP, Marques HM (2012) *cis* influence in models of cobalt corrins by DFT and TD-DFT studies. J Phys Chem B 116:8836–8845. https://doi.org/10.1021/jp304007a
20. Zelder F, Sonnay M, Prieto L (2015) Antivitamins for medicinal applications. ChemBioChem 16:1264–1278. https://doi.org/10.1002/cbic.201500072
21. Brenig C, Mestizo PD, Zelder F (2022) Functionalisation of vitamin B_{12} derivatives with a cobalt β-phenyl ligand boosters antimetabolite activity in bacteria. RSC Adv 12:28553–28559. https://doi.org/10.1039/D2RA05748D
22. Xia L, Cregan AG, Berben LA, Brasch NE (2004) Studies on the formation of glutathionylcobalamin: any free intracellular aquacobalamin is likely to be rapidly and irreversibly converted to glutathionylcobalamin. Inorg Chem 43:6848–6857. https://doi.org/10.1021/ic040022c
23. Hannibal L, Axhemi A, Glushchenko AV, Moreira ES, Brasch NE, Jacobsen DW (2008) Accurate assessment and identification of naturally occurring cellular cobalamins. Clin Chem Lab Med 46:1739–1746. https://doi.org/10.1515/CCLM.2008.356
24. Jeong J, Park J, Park J, Kim J (2014) Processing of glutathionylcobalamin by a bovine B_{12} trafficking chaperone bCblC involved in intracellular B12 metabolism. Biochem Biophys Res Commun 443:173–178. https://doi.org/10.1016/j.bbrc.2013.11.075
25. Kim J, Hannibal L, Gherasim C, Jacobsen DW, Banerjee R (2009) A human vitamin B_{12} trafficking protein uses glutathione transferase activity for processing alkylcobalamins. J Biol Chem 284:33418–33424. https://doi.org/10.1074/jbc.M109.057877
26. Calafat AM, Marzilli LG (1993) Investigations of B12 derivatives with inorganic ligands using 2D NMR spectroscopy. Ligand responsive shifts suggest that the deoxyadenosyl moiety in coenzyme B12 has a steric trans influence. J Am Chem Soc 115:9182–9190. https://doi.org/10.1021/ja00073a037
27. Zhou K, Zelder F (2011) One-step synthesis of α/β cyano-aqua cobinamides from vitamin B12 with Zn(II) or Cu(II) salts in methanol. J Porphyr Phthalocyanines 15:555–559. https://doi.org/10.1142/S1088424611003446
28. Zhou K, Zelder F (2011) Identification of diastereomeric cyano-aqua cobinamides with a backbone-modified vitamin B12 derivative and with 1H NMR spectroscopy. Eur J Inorg Chem. https://doi.org/10.1002/ejic.201001146
29. Munegumi T (2013) Where is the border line between strong acids and weak acids? World J Chem Edu 1:12–16
30. Liu M, Mao X, Ye C, Huang H, Nicholson JK, Lindon JC (1998) Improved WATERGATE pulse sequences for solvent suppression in NMR spectroscopy. J Magn Res 132:125–129. https://doi.org/10.1006/jmre.1998.1405
31. Rabenstein DL (1973) Nuclear magnetic resonance studies of the acid-base chemistry of amino acids and peptides. I. Microscopic ionization constants of glutathione and methylmercury-complexed glutathione. J Am Chem Soc 95:2797–2803. https://doi.org/10.1021/ja00790a009
32 Dereven'kov IA, Salnikov DS, Shpagilev NI, Makarov SV, Tarakanova EN (2012) Reactions of cobinamide with glucose and fructose. Macroheterocycles 5:260–265. https://doi.org/10.6060/mhc2012.120884m

33 Dereven'kov IA, Osokin VS, Molodtsov PA, Makarova AS, Makarov SV (2022) Effect of complexation between cobinamides and bovine serum albumin on their reactivity toward cyanide. React Kinet Mech Catal 135:1469–1483. https://doi.org/10.1007/s11144-022-02216-8
34. Sobornova VV, Belov KV, Dyshin AA, Gurina DL, Khodov IA, Kiselev MG (2022) Molecular dynamics and nuclear magnetic resonance studies of supercritical CO_2 sorption in poly(methyl methacrylate). Polymers 14:5332. https://doi.org/10.3390/polym14235332
35. Singh K, Kumar SP, Blümich B (2019) Monitoring the mechanism and kinetics of a transesterification reaction for the biodiesel production with low field ^{1}H NMR spectroscopy. Fuel 243:192–201. https://doi.org/10.1016/j.fuel.2019.01.084
36. Carneiro de Oliveira J, Laborie M-P, Roucoules V (2020) Thermodynamic and kinetic study of diels-alder reaction between furfuryl alcohol and *N*-hydroxymaleimides—an assessment for materials application. Molecules 25:243. https://doi.org/10.3390/molecules25020243
37. Izatt RM, Christensen JJ, Pack RT, Bench A (1962) Thermodynamics of metal-cyanide coordination. I. pK, ΔH^0, and ΔS^0 values as a function of temperature for hydrocyanic acid dissociation in aqueous solution. Inorg Chem 1:828–831. https://doi.org/10.1021/ic50004a022
38 Hamza MSA, Zou X, Brown KL, van Eldik R (2002) Detailed kinetic and thermodynamic studies on the cyanation of alkylcobalamins. A generalized mechanistic description. J Chem Soc Dalton Trans. https://doi.org/10.1039/B206706D
39. Brown KL, Hakimi JM, Jacobsen DW (1984) Heteronuclear NMR studies of cobalamins. 3. Phosphorus-31 NMR of aquocobalamin and various organocobalamins. J Am Chem Soc 106:7894–7899. https://doi.org/10.1021/ja00337a043
40. Brown KL, Hakimi JM (1984) Heteronuclear NMR studies of cobalamins. 2. Carbon-13 and phosphorus-31 NMR studies of [13C]cyanocobalamin. Inorg Chem 23:1756–1764. https://doi.org/10.1021/ic00180a022
41 Dereven'kov IA, Shpagilev NI, Makarov SV (2018) Mechanism of the reaction between cobalamin(II) and periodate. Russ J Phys Chem A 92:2182–2186. https://doi.org/10.1134/S0036024418110080
42. Lexa D, Savéant JM (1983) The electrochemistry of vitamin B12. Acc Chem Res 16:235–243. https://doi.org/10.1021/ar00091a001
43. Hinze R-P, Schiebel HM, Laas H, Heise K-P, Gossauer A, Inhoffen HH, Ernst L, Schulten H-R (1979) Beiträge zur Kenntnis des chromophoren Systems der Corrine, IV. Über die partielle, reversible Ringöffnung am Dicyano-cobyrinsäure-heptamethylester mit intermediärer reversible Entfernung des Cobalts. Liebigs Ann Chem 1979:811–825. https://doi.org/10.1002/jlac.197919790611

Authors and Affiliations

Ilia A. Dereven'kov[1] · Vladimir S. Osokin[1] · Ilya A. Khodov[2] · Valentina V. Sobornova[2] · Nikita A. Ershov[1] · Sergei V. Makarov[1]

✉ Ilia A. Dereven'kov
derevenkov_ia@isuct.ru; derevenkov@gmail.com

[1] Department of Food Chemistry, Ivanovo State University of Chemistry and Technology, Sheremetevskiy Str. 7, 153000 Ivanovo, Russia

[2] G.A. Krestov Institute of Solution Chemistry, Russian Academy of Sciences, 153045 Ivanovo, Russia